Published in final edited form as:
J Biomed Mater Res A. 2009 September 15; 90(4): 1198–1205. doi:10.1002/jbm.a.32160.

Modulating human connective tissue progenitor cell behavior on cellulose acetate scaffolds by surface microtextures

Eun Jung Kim[1,2], **Cynthia A. Boehm**[1,3], **Aaron J. Fleischman**[1], **George F. Muschler**[1,3], **Yordan V. Kostov**[4], and **Shuvo Roy**[1]

[1]BioMEMS Laboratory, Department of Biomedical Engineering, Lerner Research Institute, Cleveland Clinic, 9500 Euclid Avenue, Cleveland, Ohio 44195

[2]Department of Applied Biomedical Engineering, Cleveland State University, 2121 Euclid Avenue, Cleveland, Ohio 44115

[3]Orthopaedic Research Center, Lerner Research Institute, Cleveland Clinic, 9500 Euclid Avenue, Cleveland, Ohio 44195

[4]Department of Chemical and Biochemical Engineering, University of Maryland Baltimore County, 5200 Westland Boulevard, Baltimore, Maryland 21227

Abstract

Soft lithography techniques are used to fabricate cellulose acetate (CA) scaffolds with surface microtextures to observe growth characteristics of the progeny of human marrow-derived connective tissue progenitor cells (CTPs). Human CTPs were collected and cultured on CA scaffolds comprised postmicrotextures and smooth surfaces for up to 30 days. Cells on the smooth surfaces migrated without any preferred orientation for up to 30 days. On microtextures, cells tended to direct their processes toward posts and other cells on day 9. By day 30, cells on microtextures covered the surface with extracellular matrix. DNA quantification revealed approximately threefold more cells on microtextures than on the smooth surfaces. The alkaline phosphatase (AP) mRNA expression was slightly higher on smooth surfaces on day 9. However, by day 30, AP mRNA showed higher expression on microtextures. The mRNA expression of collagen type I was increased on microtextures by day 30, whereas smooth surfaces demonstrated similar expression. The osteocalcin mRNA expression was increased on postmicrotextures relative to smooth surfaces by day 30.

Keywords

cellulose acetate; microfabrication; soft lithography; connective tissue progenitor cells; surface topography; MEMS

Correspondence to: S. Roy; roys@ccf.org.

Introduction

Understanding cell behavior during osteogenesis and the relationship between osteoprogenitor cells and an osteoconductive scaffold is important in bone tissue engineering. An effective osteoconductive scaffold promotes new tissue formation by providing a surface that directly or indirectly promotes attachment, proliferation, migration, and desired differentiation of cells throughout the region where new tissue is needed.[1–3] At the interface of cell and scaffold surface, properties such as chemical composition, surface energy, and structural topography profoundly affect the overall behavior of the engineered cell and tissue.[3,4] Numerous studies have been conducted to show that surface topographies influence morphology, proliferation, migration, and differentiation of cells.[5–12]

Microfabrication and related MEMS (microelectro-mechanical systems) techniques enable precise production of surface topographical features, which can be used to investigate the effects of topographic cues on cellular behavior.[6,7,10] This technology could be conceptually combined with scaffold processing to ultimately provide tissue-engineering scaffolds that possess topographical, spatial, and chemical properties to optimize control over cellular behavior. In oust previous study,[9] human bone marrow-derived connective tissue progenitor cells (CTPs) were cultured for 9 days on smooth polydimethysiloxane (PDMS) surfaces and on PDMS postmicrotextures that were 6 μm high and 5, 10, 20, and 40 μm in diameter and separation, respectively. Cells on PDMS postmicrotextures demonstrated modified morphology and enhanced proliferation compared to cells cultured on smooth PDMS and control surfaces. In particular, our investigations showed that 10-μm diameter posttextures significantly enhanced CTP growth.

PDMS is accepted as a nontoxic, highly inert, ubiquitous, inexpensive, and biocompatible material.[6–8] However, it is not biodegradable, and therefore, not a universally suitable biomaterial for all tissue-engineering systems.[1] The desire for a biocompatible and biodegradable material motivated us to explore cellulose acetate (CA) as a scaffold material for tissue-engineering applications.[13–21] CA is not only a biocompatible and biodegradable material, but it also lends itself to the molding of very fine (nano and microscale structures) and intricate features.[20] CA is also known to be nontoxic, transparent, and inexpensive.[13,14] In typical processing of CA, acetone is used as a solvent. Afterward, the acetone is evaporated and CA is then treated with NaOH or water. This deacetylation reaction allows for deep penetration of water into CA and removes the remaining traces of acetone. In contrast, other materials such as polystyrene and poly(methyl methacrylate) need solvents (e.g., chloroform and toluene) that are immiscible with water.[22] Accordingly, it is difficult to remove them, and some amount of the solvent remains trapped in the material, which might degrade their biocompatibility. These characteristics make CA a favorable material to use for tissue-engineering investigations. Many reports[17–21] have confirmed that CA or cellulose-based materials are well suited for optimization and control of cell adhesion. More specifically, Martson et al. and Takata et al.[17,18] showed that cellulose-derived scaffolds exhibited a favorable bony response and rapidly formed initial “connective tissue” around scaffolds.

To increase the understanding of osteoblastic progenitor cell and scaffold surface behavior, we cultured human bone marrow cells containing CTPs on CA substrates comprised both postmicrotextures and smooth surfaces for 9 and 30 days. CTPs are defined as a heterogeneous population of cells in native tissues that can be induced to proliferate and produce progeny that differentiate into one or more connective tissue phenotypes (e.g., bone, cartilage, muscle, and fat). Bone marrow-derived CTPs, which cultured under osteogenic conditions, will generate colonies of progeny that exhibit osteogenic differentiation.[23] The differentiated osteoblast is generally characterized by a specific pattern of gene expression such as alkaline phosphatase (AP), collagen type I (Col I), osteocalcin (OC), and by *in vitro* mineralization capacity.[23–25] An investigation into the proliferation and osteogenic differentiation of CTP progeny in primary culture on CA postmicrotextures should provide a valuable model in which to explore the relationship between adult stem cell behavior and critical topographical parameters in the engineering of bone scaffolds for the enhancement of bone fracture healing.

Materials and Methods

Substrate Preparation

The microfabricated CA scaffold was manufactured by soft lithography techniques (Fig. 1). Briefly, a 6-μm thick layer of SU-8 2010 photoresist was coated on top of a silicon (Si) wafer. By using ultraviolet (UV) photolithography, the 10-μm diameter and 6-μm height texture pattern were transferred from a photomask onto the photoresist, which was then developed and cured at 120°C. CA was prepared by mixing 1-g powder-type CA (Aldrich Chemical, Milwaukee, WI) and 13 mL of spectroscopic grade acetone (Aldrich Chemical) for 2 h to obtain a clear solution. The CA mixture was poured onto the patterned SU-8 mold and dried slowly for 24 h at room temperature. Afterward, the cured CA cast was released from the mold and sectioned into 2 × 2 cm samples [Fig. 2(a)]. Partial hydrolysis and deacetylization were applied to the CA scaffolds using 100 m*M* NaOH for 24 h at room temperatures. Representative samples were inspected by scanning electron microscopy (SEM; JSM-5310, JEOL, USA; Peabody, MA). An unpatterned SU-8 substrate was used to produce smooth CA surfaces [Fig. 2(b)], and standard tissue culture glass slides (Lab-Tek Chamber Slide System, Nalge Nunc International, Naperville, IL) were served as the control. The CA scaffolds were placed inside a standard tissue culture dishes (Lab-Tek Chamber Slide System).

Cell culture

As described by Muschler et al.,[24] human bone marrow aspirates were harvested from the anterior iliac crest with informed consent from four patients immediately before elective orthopedic procedures. Briefly, 2 mL samples of bone marrow were aspirated from the anterior iliac crest into 1 mL of saline-containing 1000 U of heparin (Vector, Burlingame, CA). The heparinized marrow sample was suspended into 20 mL of heparinized carrier media (α-minimal essential medium (α-MEM) + 2 U/mL of Na-heparin; Gibco, Grand Island, NY) and centrifuged at 1500 rpm (400×g) for 10 min. The buffy coat was collected, resuspended in 20 mL of 0.3% bovine serum albumin-MEM (Gibco), and the number of nucleated cells was counted. The CA scaffolds and control substrate were sterilized for 30

min with 70% ethanol and washed several times with phosphate buffered saline (PBS) (Cambrex Bio-Science, Walkersville, MD). Cells were then plated on day 0 at a seeding concentration of 1×10^6 cells per well (2 × 2 cm) and cultured for 9 and 30 days under conditions promoting osteoblastic differentiation.[24] In this study, the PicoGreen DNA quantification was repeated three times, and real-time RT-PCR was repeated four times as per our standard laboratory protocols and convenience. We analyzed the RT-PCR results for both three repeat and four repeat data sets and noted that the change in expression levels was not statistically significant.

Cell-culture analysis

Scanning electron microscopy—On days 9 and 30, the media were removed and the plated substrates were placed in a solution containing 2% glutaraldehyde (Electron Microscopy Sciences, Fort Washington, PA), 3% sucrose (Sigma-Aldrich, Irvine, UK), and 0.1*M* PBS at 4°C and pH 7.4. After 1 h, the substrates were rinsed twice with the PBS for 30 min at 4°C and washed with distilled water for 5 min. Dehydration was achieved by placing the plated substrates in 50% ethanol for 15 min while increasing the concentration of ethanol to 60, 70, 80, 90, and finally 100%. Dehydrated samples were then critical point-dried, mounted on aluminum stubs, sputter-coated with gold–palladium, and examined using SEM.

PicoGreen DNA quantification—CTP-seeded CA scaffolds and control substrate were resuspended with 50 μL of lysis buffer (1% sodium dodecyl sulfate, 10 m*M* ethylenediaminetetraacetic acid (EDTA), and 50 m*M* Tris–HCl, pH 8.1) (Sigma-Aldrich) to lyse the membrane of adherent CTP progeny. After 60 min, the samples were centrifuged at 14,000 rpm for 5 min, and the supernatant was removed for analysis. A 40-μL sample of aqueous supernatant-containing DNA was added to 0.96-mL TE buffer (Molecular Probes, Eugene, OR). As per the manufacturer's instructions (Molecular Probes), stock PicoGreen reagent was diluted to 1:200 in TE buffer and 1 mL of that was added to each DNA-containing sample. The tubes were capped, vortexed, and incubated at room temperature in the dark room for 3 min. The fluorescence was measured with a SpectraMax Gemini fluorescence microplate reader (Molecular Devices, Sunnyvale, CA) at excitation and emission wavelengths of 480 and 520 nm, respectively. All calibration samples were assayed four times, and a fresh calibration curve was generated for each 96 well plate. Baseline fluorescence was determined with a TE blank, the average of which was subtracted from the averaged fluorescence of other samples. Using this analysis, we determined that ~ 4.5 μg of DNA in 1×10^6 adherent CTPs. Thus, we assumed that one cell has ~ 4.5 pg of DNA and estimated the number of cells for each sample. Because individual donors differed with respect to the initial prevalence of CTPs, the cell count on the CA substrates was normalized to the control surfaces for each donor within the particular experiment.

DAPI stain—Cell nuclei were stained with 6-diamidino-2-phenylindole dihydrochloride hydrate (DAPI). Ethanol-fixed cells were rinsed three times with PBS, and then a 10-μL drop of DAPI-containing Vectashield mounting media (Vector Labs, Burlingame, CA) was placed on the scaffolds. Immediately thereafter, the edges of the coverslips were sealed with three coats of clear nail polish and viewed under a fluorescent microscope (Olympus BX50F, Olympus Optical, Japan).

Alkaline phosphatase stain—After DAPI staining, the same samples were again stained *in situ* for AP, using the Vector Red substrate, working solution (5 mL of 100 m*M* Tris–HCl adding two drops of reagents 1, 2, and 3) (Vector Labs) for 30 min at room temperature in the dark and then washed in distilled water. The positively stained cells with AP activity appeared red when viewed under a fluorescent microscope.

von Kossa stain—The cells were rinsed with PBS and fixed in 4% paraformaldehyde (Electron Microscopy Sciences) for 1 h. They were then incubated in 5% silver nitrate (Sigma-Aldrich) for 30 min in the dark, rinsed with distilled water, and exposed to ultraviolet light for 1 h. Secretion of calcified extracellular matrix (ECM) was confirmed visually by the presence of deep blue-purple nodules under a phase contrast microscope.

Real-time reverse transcript-polymerase chain reaction—To quantify expressions of osteoblast-specific genes such as AP, Col I, and OC, real-time reverse transcript-polymerase chain reaction (RT-PCR) was performed. Total cellular RNA was isolated using RNeasy kit (Qiagen, Valencia, CA) and reverse transcribed by conventional protocols with a Sensiscript Reverse Transcription kit (Qiagen). Expression of the AP, Col I, OC, and glyceraldehyde-3-phosphate dehydrogenase (GAPDH) was quantified using real-time RT-PCR analysis with Power SYBR® Green PCR Master Mix kit (Applied Biosystems, Foster City, CA). GAPDH is an enzyme used in cellular metabolism and is assumed to be expressed at the same level in most cells; therefore, gene expression of GAPDH was used as an internal control to normalize out any differences in the amount of total RNA isolated.[25] Primer sequences are presented in Table I. Real-time quantitative PCR was performed on a 7500 real-time PCR system (Applied Bio-systems). Data analysis was carried out using the 7500 System Sequence Detection software (Applied Biosystems).[26]

Statistical analysis

The mean and standard error values were calculated using the data of all groups. All data were subjected to analysis of variance (ANOVA) and Tukey testing where appropriate (SPSS Version 10.0) (SPSS, Chicago, IL). Significance levels were set at $p < 0.05$.

Results

Morphology

The SEM images revealed that human CTPs attached to CA postmicrotextures, smooth CA, and control surfaces with varying cell morphology (Fig. 3). Cells on the smooth and control surfaces exhibited arbitrary flattened shapes and migrated without any preferred orientation for up to 30 days. In contrast, CTPs on postmicrotextures on day 9 mostly tended to attach next to the posts and spread between them while directing their processes toward posts and other cells. By day 30, numerous cells had spread over the top of the CA postmicrotextures and covered most of the surface with ECM.

Cell proliferation

Using DNA quantification analysis, the corresponding numbers of CTPs were calculated (Fig. 4). CA postmicrotextures exhibited a greater number of CTPs compared to smooth CA

and control surfaces. On days 9 and 30, CA postmicrotextures supported a greater cell number than smooth CA and control surfaces ($p < 0.05$). The CTPs on scaffolds were viewed by DAPI staining (Fig. 5). Cell nuclei were stained with DAPI and qualitatively confirmed that there are more cells on posttextures than smooth and control surfaces by day 30.

ECM expression

Cells on all scaffolds stained positive for AP, which is used as a marker of osteoblast phenotype (Fig. 5). Cells on the CA postmicrotextures stained more intensely for AP compared to smooth CA and control surfaces on day 9, and AP increased on all scaffolds by day 30. The von Kossa stain exhibited minimal intensity on all scaffolds on day 9 but increased greatly by day 30, especially on the CA postmicrotextures. Furthermore, the coverage and intensity of von Kossa stain on CA postmicrotextures were increased compared to the smooth CA and control surfaces [Fig. 5(b)]. These results indicated that bone mineralization had started at day 9 and increased immensely over time, but more especially so, on the CA postmicrotextures.

Gene expression

Using CTPs obtained from each scaffold, we examined gene expression of the key osteoblastic bone markers, such as AP, Col I, OC, and the well-documented housekeeping gene *GAPDH*, over a period of 9 and 30 days (Fig. 6). The results of real-time RT-PCR revealed that AP mRNA expression was not different between CA microtextures and smooth surfaces on day 9 [Fig. 6(a)]. In contrast, the mRNA expression of AP had increased by day 30 on postmicrotextures ($p < 0.05$), but not on smooth surfaces. On day 9, Col I mRNA expression on both postmicrotextures and smooth surfaces is similar [Fig. 6(b)]. The mRNA expression of Col I was increased on postmicrotextures by day 30, but there was no increase in the expression of Col I mRNA on smooth surfaces. Finally, the OC mRNA expression was increased on postmicrotextures relative to smooth surfaces ($p < 0.05$) by day 30 [Fig. 6(c)].

Discussion

This study has shown that postmicrotextures on CA scaffolds enhance proliferation as well as matrix and mineral secretion by osteogenic progeny of CTPs *in vitro*. DNA analysis revealed a greater number of cells on CA postmicrotextures than on smooth CA and control surfaces (Fig. 4). This result is consistent with our previous study,[9] where CTP progeny cultured on PDMS postmicrotextures also exhibited increased cell number relative to smooth and control surfaces.

Increased cell proliferation suggests that the CA postmicrotextures provide favorable growth conditions. According to our previous experiments with PDMS substrates,[9] the number of CTPs attached initially on postmicrotextures and smooth surfaces are almost identical. This observation suggested that CTP attachment was not preferentially enhanced, but rather, there was an increased proliferation on the postmicrotextures. Therefore, it is likely that the difference in cell proliferation on postmicrotextures and smooth surfaces is due reduction in

lag time between initial cell contact with the substrate surface and cell spreading. The earlier onset of proliferation would result in increased cell number on days 9 and 30, which would be consistent with our observations as an apparent shortening of cell-cycle time. Dobereiner et al.[27] have established that the onset of cell spreading is characterized by an increase in actin polymerization, which is triggered by favorable contact with the ECM. Furthermore, Dubin-Thaler et al.[28] have reported that the length of time lag between cell contact with ECM molecules and onset of cell spreading was inversely related to ECM molecule concentration. In our investigation, the microtextures also increased surface area under a cell relative to the smooth surfaces. Separation of effects of ECM molecular density and surface area on cell proliferation from those resulting from microtextures will require additional investigation.

As observed in this study, CA postmicrotextures resulted in an increase in markers of osteoblastic differentiation including AP activity as well as expression of Col I and OC. This evidence is also consistent with the findings reported by Healy et al.[5] and Hamilton et al.[10] who found that microfabricated surfaces influenced osteoblastic differentiation *in vitro*. Although a slight increase may be present, the increase in OC was not statistically significant. Additional investigation will be needed to determine possible reasons. Also, future investigations will be required to assess the effects of surface microtextures on other important aspects of cellular kinetics during osteogenesis, including cell-cycle time, apoptosis, detachment, migration, and deposition of extracellular calcium.

Unlike PDMS, the biodegradability of CA makes it more attractive as an osteoconductive structural material for bone fracture healing. However, CA has been reported to exhibit limited degradation rates.[20] We experimentally confirmed the slow degradation rate (<5% of original weight) of our CA substrates after 10 weeks of immersion in saline solution (data not shown). To increase the degradation rate, the CA can be converted to cellulose during cell growth or before implantation using the cellulose enzyme.[20] Cellulose is nonimmunogenic and, upon biodegradation, the final product is glucose. Accordingly, future studies will be required to confirm *in vitro* and *in vivo* applicability of converted cellulose and its effects on CTP progeny.

Conclusion

Microfabrication enables reproducible patterning of precise surface microtextures that can be exploited to investigate cellular response to surface morphology. The information obtained from such investigations is particularly crucial to the successful development of scaffolds for bone tissue engineering. We have shown that culturing primary bone marrow-derived human CTPs and their progeny under osteogenic conditions on CA postmicrotextures enhances proliferation and differentiation compared to that on smooth CA and control surfaces. The results demonstrate a significant response of osteogenic CTPs to topography and suggest a practical role for CA post-textured materials in modifying the behavior of osteogenic cells. Knowledge of the response of osteogenic cells to surface stimuli could lead to the incorporation of specific microtextures into surfaces of bone implants and scaffolds used to enhance fracture healing.

Acknowledgments

The authors thank Anna Dubnisheva and Illya Gordon, both of the Cleveland Clinic, for their assistance.

Contract grant sponsor: NIH; contract grant number: R01 AR42997

Contract grant sponsor: NIH Musculoskeletal Core Center, Cleveland Clinic

References

1. Ratner BD, Bryant SJ. Biomaterials: Where we have been and where we are going. Annu Rev Biomed Eng. 2004; 6:41–75. [PubMed: 15255762]
2. Curtis A. Nanofeaturing materials for specific cell responses. Mater Res Soc Symp Proc. 2005; 845:175–184.
3. Muschler GF, Nakamoto C, Griffith LG. Engineering principles of clinical cell-based tissue engineering. J Bone Joint Surg A. 2004; 86:1541–1558.
4. El-Amin SF, Botchwey E, Tuli R, Kofron MD, Mesfin A, Sethuraman S, Tuan RS, Laurencin CT. Human osteoblast cells: Isolation, characterization, and growth on polymers for musculoskeletal tissue engineering. J Biomed Mater Res A. 2006; 76:439–449. [PubMed: 16541483]
5. Healy KE, Thomas CH, Rezania A, Kim JE, McKeown PJ, Lom B, Hockberger PE. Kinetics of bone cell organization and mineralization on materials with patterned surface chemistry. Biomaterials. 1996; 17:195–208. [PubMed: 8624396]
6. Raghavan S, Chen CS. Micropatterned environments in cell biology. Adv Mater. 2004; 16:1303–1313.
7. Chen CS, Jiang X, Whitesides GM. Microengineering the environment of mammalian cells in culture. MRS Bull. 2005; 30:194–201.
8. Chen CS, Tan J, Tien J. Mechanotransduction at cell-matrix and cell-cell contacts. Annu Rev Biomed Eng. 2004; 6:275–302. [PubMed: 15255771]
9. Mata A, Boehm C, Fleischman AJ, Muschler G, Roy S. Growth of connective tissue progenitor cells on microtextured polydimethylsiloxane surface. J Biomed Mater Res. 2002; 62:499–506. [PubMed: 12221697]
10. Hamilton DW, Wong KS, Brunette DM. Microfabricated discontinuous-edge surface topographies influence osteoblast adhesion, migration, cytoskeletal organization, and proliferation and enhance matrix and mineral deposition in vitro. Calcif Tissue Int. 2006; 78:314–325. [PubMed: 16604286]
11. Deutsch J, Motlagh D, Russell B, Desai TA. Fabrication of microtextured membrane for cardiac myocyte attachment and orientation. J Biomed Mater Res. 2000; 53:267–275. [PubMed: 10813767]
12. Anselme K. Osteoblast adhesion on biomaterials. Biomaterials. 2000; 21:667–681. [PubMed: 10711964]
13. Liu H, Hsieh YL. Ultrafine fibrous cellulose membranes from electrospinning of cellulose acetate. J Polym Sci Part B: Polym Phys. 2002; 40:2119–2129.
14. Miyamoto T, Takahashi S, Ito H, Inagaki H, Noishiki Y. Tissue biocompatibility of cellulose and its derivatives. J Biomed Mater Res. 1989; 23:125–133. [PubMed: 2708402]
15. Martson M, Viljanto J, Hurme T, Laippala P, Saukko P. Is cellulose sponge degradable or stable as implantation material? An in vivo subcutaneous study in the rat. Biomaterials. 1999; 20:1989–1995. [PubMed: 10535810]
16. Sevillano G, Rodriguez-Puyol M, Martos R, Duque I, Lamas S, Diez-Marques ML. Cellulose acetate membrane improves some aspects of red blood cell function in haemodialysis patients. Nephrol Dial Transpl. 1990; 5:497–499.
17. Martson M, Viljanto J, Hurme T, Saukko P. Biocompatibility of cellulose sponge with bone. Eur Surg Res. 1998; 30:426–432. [PubMed: 9838236]
18. Takata T, Wang HL, Miyauchi M. Migration of osteoblastic cells on various guided bone regeneration membranes. Clin Oral Implants Res. 2001; 12:332–338. [PubMed: 11488862]

19. Laiuppa JA, McAdams TA, Papoutsakis ET, Miller WM. Culture materials affect ex vivo expansion of hematopoietic progenitor cells. J Biomed Mater Res. 1997; 36:347–359. [PubMed: 9260106]

20. Entcheva E, Bien H, Yin L, Chung CY, Farrell M, Kostov Y. Functional cardiac cell constructs on cellulose-based scaffolding. Biomaterials. 2004; 25:5753–5762. [PubMed: 15147821]

21. Cullen B, Watt PW, Lundqvist C, Silcock D, Schmidt RJ, Bogan D, Light ND. The role of oxidised regenerated cellulose/collagen in chronic wound repair and its potential mechanism of action. Int J Biochem Cell Biol. 2002; 34:1544–1556. [PubMed: 12379277]

22. Okubo M, Saito N, Fujibayashi T. Preparation of polystyrene/poly(methyl methacrylate) composite particles having a dent. Colloid Polym Sci. 2005; 283:691–698.

23. Muschler GF, Midura RJ. Connective tissue progenitors: Practical concepts for clinical applications. Clin Orthop Relat Res. 2002; 395:66–80. [PubMed: 11937867]

24. Muschler GF, Nitto H, Boehm CA, Easley KA. Age- and gender-related changes in the cellularity of human bone marrow and the prevalence of osteoblastic progenitors. J Orthop Res. 2001; 19:117–125. [PubMed: 11332607]

25. Tsigkou O, Hench LL, Boccaccini AR, Polak JM, Stevens MM. Enhanced differentiation and mineralization of human fetal osteoblasts on PDLLA containing Bioglass composite films in the absence of osteogenic supplements. J Biomed Mater Res A. 2007; 80:837–851. [PubMed: 17072851]

26. Cool SM, Nurcombe V. Substrate induction of osteogenesis from marrow-derived mesenchymal precursors. Stem Cells Dev. 2005; 14:632–642. [PubMed: 16433618]

27. Dobereiner H, Dubin-Thaler BJ, Giannone G, Sheetz MP. Force sensing and generation in cell phases: Analyses of complex functions. J Appl Physiol. 2004; 98:1542–1546. [PubMed: 15772064]

28. Dubin-Thaler BJ, Giannone G, Dobereiner H, Sheetz MP. Nanometer analysis of cell spreading on matrix-coated surfaces reveals two distinct cell states and STEPs. Biophys J. 2004; 86:1794–1806. [PubMed: 14990505]

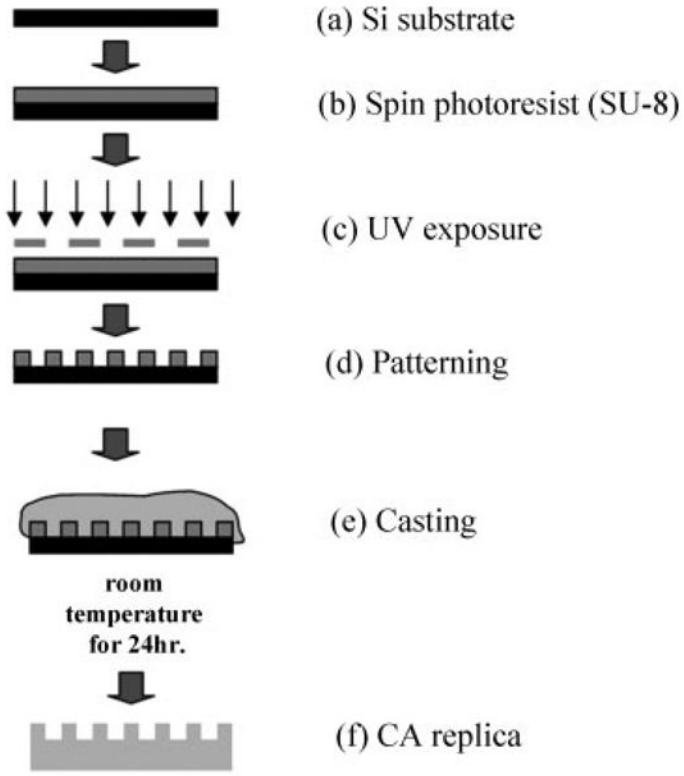

Figure 1.

Fabrication of CA postmicrotextures by soft lithography. The cross-sectional schematic diagrams depict (a) starting substrate, which is a 100-mm diameter, 500-μm thick silicon (Si) wafer; (b) a 6-μm thick layer of SU-8 2010 photoresist was spin-coated on top of the Si wafer; (c) using ultraviolet (UV) photolithography, a 10-μm diameter texture pattern was transferred from a photomask onto the photoresist; (d) developed photoresist (pattern); (e) molding of CA by casting; and (f) release of CA cast from SU-8 mold.

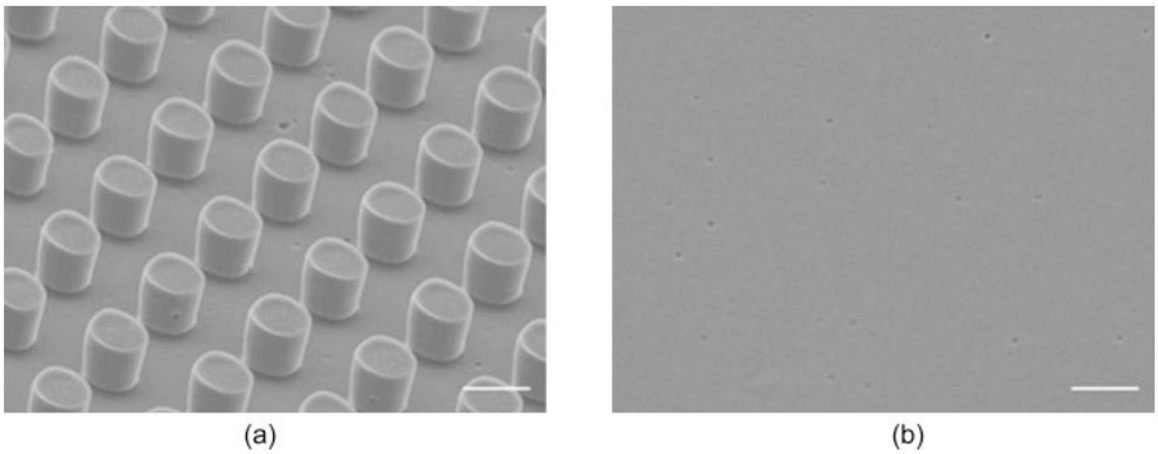

Figure 2.

SEM images of CA substrates. (a) CA postmicrotextures with posts that were 6 μm in height, 10 μm in diameter, and with 10-μm separation between posts; and (b) smooth CA surface (scale bar = 10 μm).

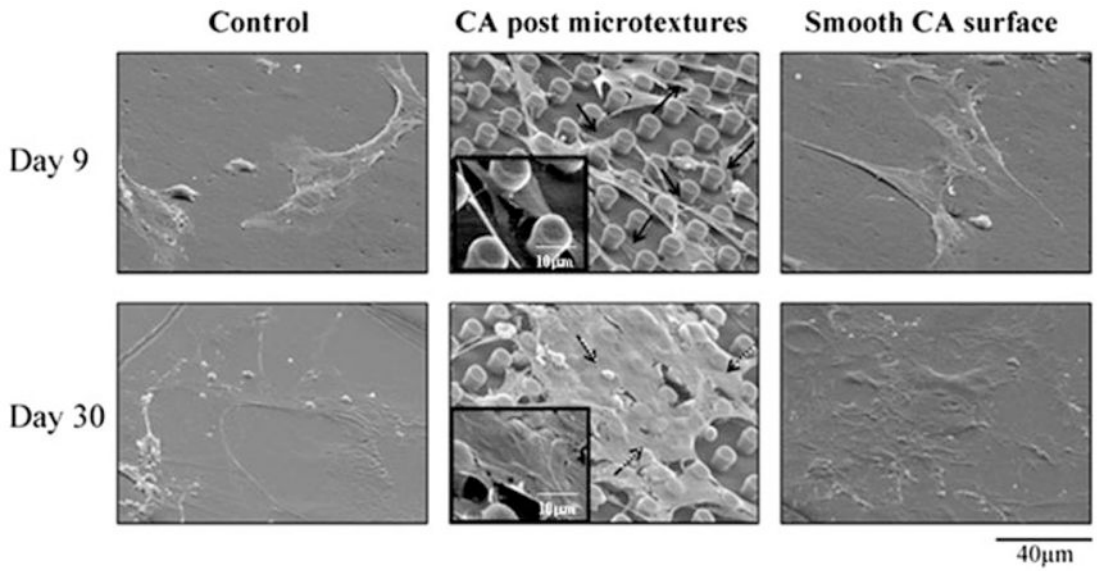

Figure 3.

SEM images of CTP progeny on CA postmicrotextures, smooth CA, and control surfaces on days 9 and 30. CTPs attached to CA postmicrotextures, smooth CA, and control surfaces with varying cell morphology. On postmicrotextures, CTPs mostly tended to attach next to the posts and spread between them while directing their processes toward posts and other cells on day 9 (solid arrows and inset). On day 30, numerous cells grew and spread over the top of the CA postmicrotextures and covered most of the surface with ECM (dashed arrows and inset). In contrast, cells on the smooth and control surfaces exhibited arbitrary flattened shapes and migrated without any preferred orientation for up to 30 days.

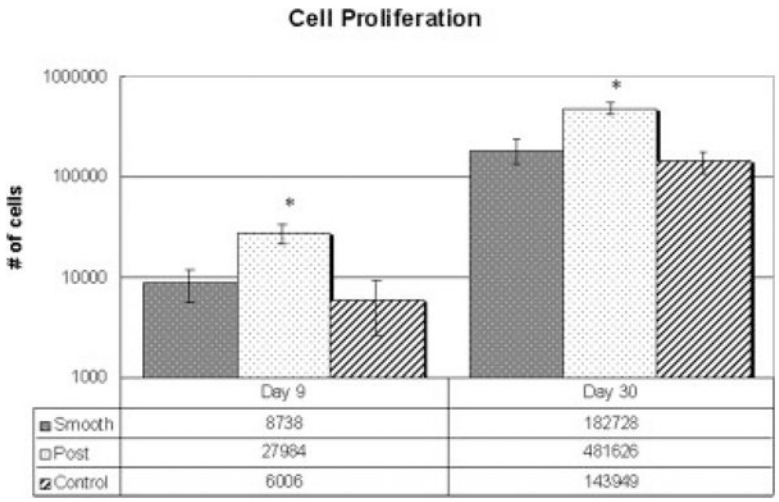

Figure 4.

CTP number on CA postmicrotextures and corresponding smooth surfaces. The PicoGreen DNA quantification was repeated thrice. CA postmicrotextures exhibited a greater number of CTPs than smooth CA and control surfaces. On days 9 and 30, there were a greater number of cells on CA postmicrotextures than on smooth CA surfaces, when compared with the control. Numerical values denote original cell number and standard errors. * denotes statistical significance compared to smooth CA surfaces and control on days 9 and 30, respectively ($p < 0.05$).

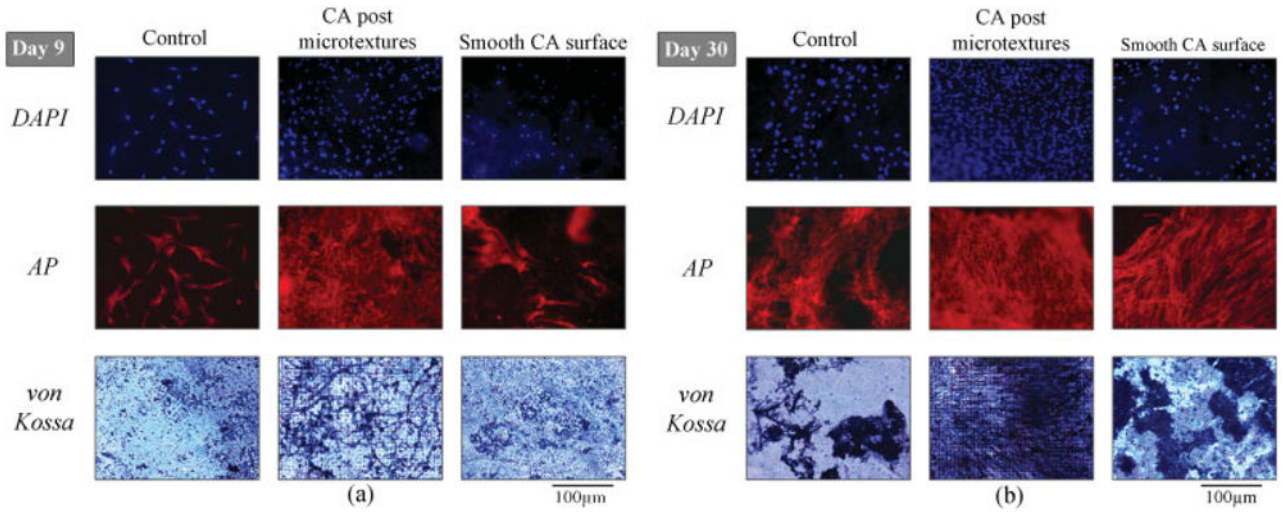

Figure 5.

Fluorescent and phase contrast microscopy images of CTPs on CA postmicrotextures, smooth CA, and control surfaces on (a) day 9 and (b) day 30. Fluorescent images show cells stained with DAPI and AP, whereas phase contrast images show von Kossa stain. Cell nuclei were stained with DAPI to qualitatively reveal more cells on postmicrotextures than smooth and control surfaces. CTPs on the CA postmicrotextures stained more intensely for AP, a marker of osteoblastic phenotype, compared to smooth CA and control surfaces on day 9, and AP increased on all scaffolds by day 30. Furthermore, the coverage and intensity of von Kossa stain on CA postmicrotextures was increased compared to the smooth CA and control surfaces. [Color figure can be viewed in the online issue, which is available at www.interscience.wiley.com.]

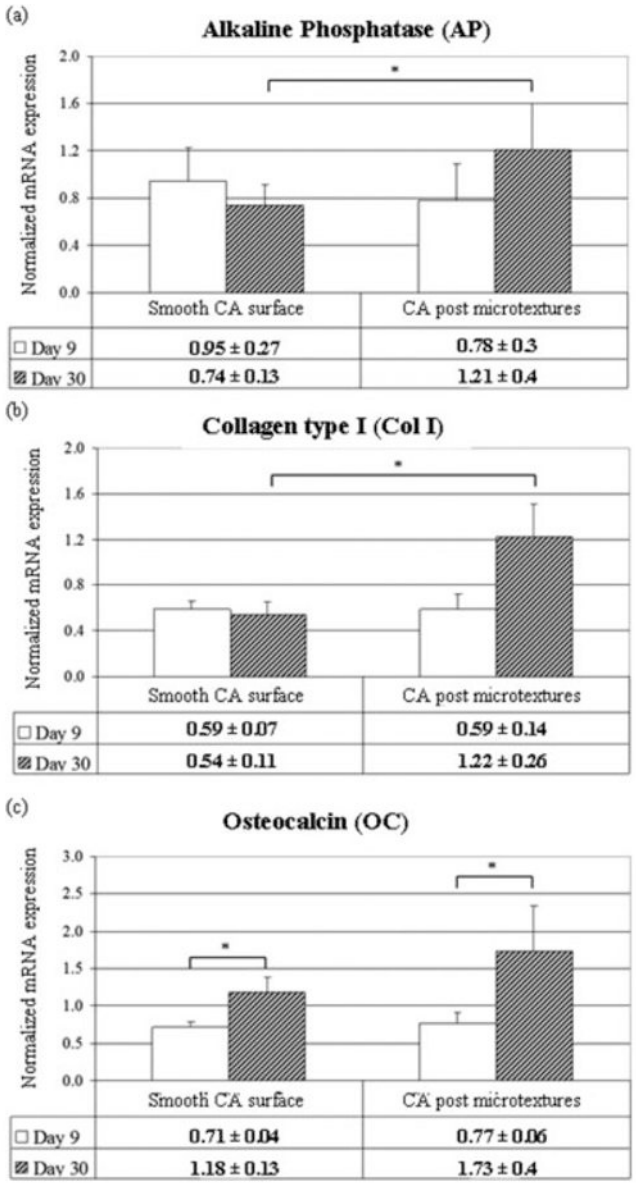

Figure 6.

mRNA expression of: (a) AP, (b) collagen type I (Col I), and (c) osteocalcin (OC) from CTPs after 9 and 30 days on CA postmicrotextures and smooth CA surfaces. The real-time RT-PCR was repeated four times, and the data are normalized to corresponding control surfaces (set to 1.0) within a particular experiment to account for differences in CTPs among individual donors. AP mRNA expressed slightly higher on day 9 compared to day 30 on smooth surfaces. In contrast, the mRNA expression of AP has increased by day 30 on postmicrotextures. On day 9, Col I mRNA expression on both postmicrotextures and smooth surfaces is similar. The mRNA expression of Col I was increased on postmicrotextures on day 30, but there was similar expression of Col I mRNA on smooth surfaces. Even though OC mRNA expression was almost the same on day 9 for both smooth and posttextured surfaces, it expressed more strongly on postmicrotextures on day 30. Numerical values denote mean and standard errors. * denotes statistical significance ($p < 0.05$).

Table I

List of Primers

Gene	Primer Sequences
Alkaline	5′ ACA GAT GCC AAC TTC CCA CAC G 3′
Phosphatase	3′ GAG GCA CCT TGT AAG ACC TAG AC 5′
Collagen	5′ CTC CAC TCC TTC CCA AAT CTG TC 3′
Type I	3′ CTT TGT AGC CTA AAC CCC TTG C 5′
Osteocalcin	5′ AGG TGC AGC CTT TGT GTC CAA G 3′
	3′ GGG AAG AAA GGA GAA GGG GAA C 5′
GAPDH	5′ GGG CTG CTT TTS SCT CTG GT 3′
	3′ TGG CAG GTT TTT CTA GAC GG 5′